

~~CONFIDENTIAL~~

Copy 208
RM L54D14

NACA RM L54D14

8538

0144277



TECH LIBRARY KAFB, NM

~~CONFIDENTIAL~~
NACA

RESEARCH MEMORANDUM

A PRELIMINARY INVESTIGATION OF THE PRESSURE RECOVERY OF
SEVERAL TWO-DIMENSIONAL SUPERSONIC INLETS

AT A MACH NUMBER OF 2.01

By Raymond J. Comenzo

Langley Aeronautical Laboratory
Langley Field, Va.

CLASSIFIED DOCUMENT

This material contains information affecting the National Defense of the United States within the meaning of the espionage laws, Title 18, U.S.C., Secs. 793 and 794, the transmission or revelation of which in any manner to an unauthorized person is prohibited by law.

**NATIONAL ADVISORY COMMITTEE
FOR AERONAUTICS**

WASHINGTON

June 23, 1954

~~CONFIDENTIAL~~

A

NO. 104 (OF 104) TO... Unclassified.....
OFFICER AUTHORIZED TO CHANGE) NASA Tech Pub Announcement #8
DATE 26 Aug. 59
GRADE OF OFFICER MAKING CHANGE) NK
DATE 9 Mar 61



NATIONAL ADVISORY COMMITTEE FOR AERONAUTICS

RESEARCH MEMORANDUM

A PRELIMINARY INVESTIGATION OF THE PRESSURE RECOVERY OF
SEVERAL TWO-DIMENSIONAL SUPERSONIC INLETS

AT A MACH NUMBER OF 2.01

By Raymond J. Comenzo

SUMMARY

A preliminary investigation of several two-dimensional supersonic inlet configurations has been conducted at the Langley Aeronautical Laboratory at a Mach number of 2.01 and an angle of attack of 0° . Two inlets similar in supersonic diffuser design but one having a subsonic diffuser approximately equal to one-half the length of the other were also investigated. Variable geometry was incorporated in the design in an attempt to obtain high values of total-pressure recovery.

Maximum values of total-pressure recovery of 0.88 and 0.83 were obtained for inlets designed for Mach numbers of 2.0 and 2.5, respectively. A 50-percent decrease in subsonic diffuser length decreased the maximum pressure recovery approximately 10 percent. Shadowgraphs indicated extensive boundary-layer separation for the case of maximum pressure recoveries.

INTRODUCTION

Various types of supersonic inlets have been investigated at and below a Mach number of 2.0 to determine the relative advantages of decelerating the free-stream air by means of a normal shock wave alone (ref. 1) or by means of a conical or two-dimensional oblique shock wave in conjunction with a normal shock wave (refs. 2 to 4). This report presents the pressure-recovery results obtained from a preliminary investigation of several two-dimensional supersonic inlets which utilized a combination of oblique and normal shock waves to decelerate the flow. The inlets tested appeared promising from theoretical calculations. In addition, a method of obtaining a short-length subsonic diffuser was also investigated. The two-dimensional inlet design consists of two wedges staggered with respect to each other and is shown in figure 1. In order to obtain high values of pressure recovery, variable geometry is

~~CONFIDENTIAL~~

incorporated in the design. Variable geometry is attained by allowing one of the wedges to be movable in a manner similar to a control surface.

The inlets were tested at a Mach number of 2.01 and at an angle of attack of 0° . Data include total-pressure recovery and shadowgraphs for each model investigated.

The inlets were designed and the test program was conducted at the Langley Laboratory under the supervision of Dr. Antonio Ferri in 1948. Because of the press of more urgent work, processing and publication of the results have been delayed. Recent increased interest in this type of inlet has made it desirable to publish the results at this time.

SYMBOLS

M_0	free-stream Mach number
M_D	design Mach number
M	Mach number
δ_w	angle of stationary wedge, deg
δ_f	angle made by surface of movable flap, nearer the stationary wedge, with respect to free-stream direction, (outward deflection of flap positive), deg
H/H_0	total-pressure-recovery ratio

MODELS AND TESTS

The investigation was made in a blowdown jet by using low-humidity air from large pressurized tanks. The Reynolds number of this investigation is 2.6×10^6 per inch.

Models.- The models consisted of a movable flap, stationary wedge, and subsonic diffuser as shown in figure 1. The movable flap was manually actuated and remotely controlled from a location near the throttling valve for convenience of operation. The stationary wedge could be changed by replacement of the entire wedge. The subsonic diffuser for the models presented in figure 1 consisted of upper and lower surfaces diverging at a total angle of 6° mounted between parallel sidewalls and included a

long minimum section for normal-shock stabilization. The width of the duct was constant for all the inlets investigated.

The boundary layer on the nozzle sidewalls was removed by decreasing the width of the nozzle blocks from 3 to 2 inches, as indicated in figure 1(c). A photograph of model 1A is presented as figure 1(d). An assembly drawing of the short-length diffuser with blades and sidewalls is shown in figure 2. The short-length diffuser had a divergence angle of 12° between the upper and lower surfaces; thus, the overall inlet length was decreased to approximately one-half that of figure 1(a). The subsonic area distributions of all models investigated are shown in figure 3.

Test procedure.- The tests were conducted in the following manner:

(1) The tunnel was started with the movable flap deflected at a high positive angle to insure that the inlet did not start. The flap angle was then decreased until the inlet started. This condition indicated the maximum contraction ratio in which the inlet would start in the fixed-geometry condition. A check was made on this contraction ratio by starting the tunnel with the flap in the position thus obtained, and in all instances the inlet started.

(2) Data were then obtained for flap angles more negative than that indicated in condition (1).

(3) Data for the inlet operating in the variable-geometry condition (flap angle greater than that of condition (1)) were obtained in the following manner: The test was started with the flap in the position obtained from condition (1), the flap deviation was increased, and at each flap position, maximum pressure-recovery data were taken. This procedure was continued during the runs until the maximum flap position at which the inlet would operate was attained. Owing to a limited air supply and the necessary rapid coordination of flap position and throttling valve, some uncertainty exists in both the maximum-pressure-recovery valve and the maximum flap position. The above doubts apply, of course, only to operation at flap angles above that of condition (1).

Measurements.- Seven total-pressure tubes and two static-pressure tubes (indicated in fig. 1(c)) were used at the rear of the diffuser of the inlet in a region of low velocity. The pressure measurements were recorded on gages and the total-pressure recovery was arithmetically averaged because no mass flow was measured. This calculation of pressure recovery was also checked by an area-weighted technique. Shadowgraphs were taken for all conditions investigated.

DISCUSSION

Inlet design.- The fact that a system of oblique shock waves results in less total-pressure loss than a normal shock at any supersonic Mach number was the primary consideration in the design of this inlet. The design-shock-wave pattern utilized in the two-dimensional inlet designs presented herein is shown in figure 4. (Letters and numbers used in this section refer to items in fig. 4.) For a free-stream Mach number M_0 , a wedge (a) produces an oblique shock wave (1) which makes contact with the lip of the movable flap (b). Another oblique shock wave (2) produced by the movable wedge coincides with the surface of wedge (a) at point (P) (fig. 4), and the surface of wedge (a) is then made parallel to the free-stream direction from point (P) to the beginning of the subsonic diffuser. In order that the inlet can operate properly, the oblique shock wave (2) that coincides with wedge (a) must be capable of being reflected from the surface of wedge (a) at point (P). Behind the oblique shock wave (2), (fig. 4) where the Mach number (M_2) is considerably lower than the free-stream Mach number (M_0), the normal shock (3) occurs (fig. 4). Numerous combinations of wedge angles and flap deflections are conceivable, and those tested are presented in figure 5, although they may not necessarily be optimum. In the design condition, the inlet attains low drag by allowing the external surfaces of the movable flap and stationary wedge to be parallel to the free-stream direction.

Inlets 1A and 2C (fig. 5) were exactly designed for low-drag and high-pressure recovery; however, the other inlets were compromise designs utilizing the available models. Thus, some expansions occur at the hinge lines which were avoided in inlets 1A and 2C.

By maintaining the supersonic design of model 1A presented in figure 5(a), an attempt was made to shorten the inlet by decreasing the length of the subsonic diffuser section. This shortening of the inlet was accomplished by allowing the subsonic diffuser to diverge at a large angle on the upper and lower surfaces of the inlet and inserting two airfoils at the entrance of the subsonic diffuser, as shown in figure 2. The airfoils were located in such a manner that the subsonic duct area increased gradually. The curved portions were placed nearer the inlet surfaces and the flat sides were facing each other, as indicated in figure 2.

Pressure recovery.- Maximum pressure-recovery data on inlets designed for $M = 2.0$ are presented in figure 6. The maximum value of pressure recovery attained was 0.88 with model 1A (fig. 6). Also presented in figure 6 is the maximum pressure-recovery values of the short-length diffuser. The data indicate that a loss in maximum pressure recovery of approximately 10 percent is obtained with the short diffuser in comparison

with the two-dimensional diffuser (model 1A) having the same supersonic design. This difference in pressure recovery appears large; however, it is believed that, with further experimentation on this method of obtaining short-length diffusers, the losses can decrease. The short vertical lines, shown in figures 6 and 7, indicate the flap angle obtained for maximum contraction ratio for the inlet operating in the fixed-geometry condition.

Figure 7 presents maximum pressure-recovery data for inlets designed for $M = 2.5$ and tested at $M = 2.01$. The maximum value of pressure recovery attained was 0.83 for model 1E (fig. 7).

Shadowgraphs.- Shadowgraphs of all models are presented in figures 8 to 10. Photographs of five different inlets are presented in figure 8, three (models 1A, 1B, and 1C) are designed for $M = 2.0$ and two (models 1D and 1E) are designed for $M = 2.5$; however, all were tested at $M = 2.01$ by utilizing the movable flap and diffuser section of model 1. In figure 8, only the supersonic portion of the inlets was enclosed in the glass section of the sidewalls. The first two photographs and of each inlet in figure 8 represent the inlet operating at different movable flap angles and at back pressure below that required for maximum pressure recovery. The third photograph of each inlet represents the last stable operating condition of the inlet. There are two positions of the normal shock in which instability occurs in the inlets investigated. When the normal shock is located in the minimum section or near the corner of the stationary-wedge surface (where the surface changes from δ_w to being parallel to the free-stream direction, point (P), fig. 3) the shock becomes unstable and moves to the lip of the movable flap and again attains equilibrium. Any attempt to move the shock farther than indicated in the shadowgraphs of figure 8 (third shadowgraphs for models 1A, 1B, 1C, 1D, and 1E) resulted in inlet buzz. Another point of interest that is clearly shown in the same shadowgraphs of figure 8 is the separation of the sidewall boundary layer that takes place ahead of the movable flap.

Figure 9 presents three different inlets utilizing the movable flap and subsonic diffuser of model 2. Two of the inlets (models 2B and 2A) are designed for $M = 2.0$ and the other (model 2C) is designed for $M = 2.5$; however, all the results are for $M = 2.01$. For model 2, a portion of the subsonic diffuser is enclosed in the glass section of the sidewalls. In figure 9(a) the shadowgraphs represent different positions of the movable flap for inlet model 2B. Figures 9(b) and 9(c) are shadowgraphs for the inlets operating at a constant flap angle and different values of back pressure. Increasing the back pressure moves the normal shock nearer the minimum section and hence increases the pressure recovery. Being able to view within the subsonic diffuser has given some insight into the phenomena that occur in inlets of this nature as the normal shock is moved into the minimum section. As can be seen in the

first shadowgraph of figure 9(b), the shock wave emanating from the movable flap coincides with the lower surface and no separation is noticeable. However, this shock wave when reflected from the stationary wedge again makes contact with the movable flap and a slight thickening of the boundary layer on the movable flap is noticeable, as indicated by the arrow. As the normal shock is moved toward the minimum section (back pressure increasing), the separation that exists on the movable flap increases and an increase in the boundary-layer thickness on the stationary wedge is also evident, as indicated in the second shadowgraph in figure 9(b). This effect of increasing boundary-layer thickness with increasing back pressure is now clearly seen in figure 9(c). As the normal shock approaches the minimum section (from the downstream end, the back pressure increasing), increased values of pressure recovery, the separation increases on the stationary wedge, as indicated by the arrow in figure 9(c).

This boundary-layer separation must also exist in the other inlets; however, only photographs of the subsonic diffuser portion of the inlets presented in figures 9(b) and 9(c) are available. Although the only separation that can be observed is seen to occur on the inlet surfaces, it is reasonable to believe that similar separation is taking place on the inlet sidewalls. Thus, it appears that separation is a cause of the reduced total-pressure recoveries as compared with the theoretical values, particularly because the pressure recoveries were averaged on an "area weighted" process rather than on a mass-flow-weighted process. It is indeed clear that, in order to approach the theoretical values of pressure recovery, some means of boundary-layer control is necessary so that the separation effects are minimized.

Figure 10 presents shadowgraphs of the short diffuser inlet operating with low and high back pressure for the same movable flap angle. The prime points of interest are that all three channels in the subsonic diffuser section started and it was possible to bring the normal shock to the entrance of the channels, although some increase in boundary-layer thickness on the inlet upper and lower surfaces is noticeable. Any attempt to move the normal shock farther into the minimum section resulted in inlet buzz.

One disadvantage of these inlets with the movable flap is that, if the inlet is operating in a condition beyond the maximum contraction ratio and something unforeseen occurs within the propulsion system that forces the normal shock out ahead of the movable flap, it would be necessary to move the flap in order to restart the inlet before it can be operated with the flap in its original position. Such a motion would give an undesirably abrupt change in mass flow and pressure recovery at the particular flight Mach number.

Although this type of inlet has indicated some promise with respect to attaining worthwhile pressure recovery, complete data on the mass flow, pressure-recovery distribution, and drag characteristics through the Mach number range are required in order to obtain some comparison with other available inlets.

Suggested inlet improvement.- In the design of the inlets presented, the inlet surfaces at the minimum section were made to follow the same direction as the free stream at $\alpha = 0^\circ$. Therefore, the compression wave (emanating from the movable flap) that coincided with the surface of the stationary wedge was required to be reflected so that the inlet would operate properly. The original design is shown by solid lines in figure 11. If the inlet surfaces at the minimum section were designed parallel to the direction of flow produced by the compression wave emanating from the lip of the movable flap (dotted lines, fig. 11), no reflection of this compression wave would be required. Hence, a lower Mach number could be obtained in the minimum section with the new design than with the original design. An improvement of this nature may increase the pressure recovery of the inlet in addition to possibly alleviating the boundary-layer separation. A change that may improve the original inlet design would be to sweep back the sidewalls coincident with the shock wave emanating from the stationary wedge. This change would decrease the entering boundary layer and prevent any shock--boundary-layer interaction with the initial shock wave.

Another improvement may be to design the inlet so that the shock--boundary-layer interaction that takes place on the stationary wedge is eliminated. This design can be accomplished by removing the boundary layer on the stationary wedge (with a bleed system); hence, the shock wave (from the movable flap) could impinge on a surface free of the boundary layer.

CONCLUDING REMARKS

A preliminary investigation has been made of several two-dimensional supersonic inlet configurations at a Mach number of 2.01 and an angle of attack of 0° . Variable geometry was incorporated in the design in an attempt to obtain high values of total-pressure recovery. Two inlets similar in supersonic diffuser design but one having a subsonic diffuser approximately equal to one-half the length of the other were investigated. The following results were obtained from this investigation:

1. For inlets designed for a Mach number of 2.0, a maximum value of total-pressure recovery of 0.88 was obtained.

2. A maximum value of total-pressure recovery of 0.83 was obtained for inlets designed for a Mach number of 2.5.

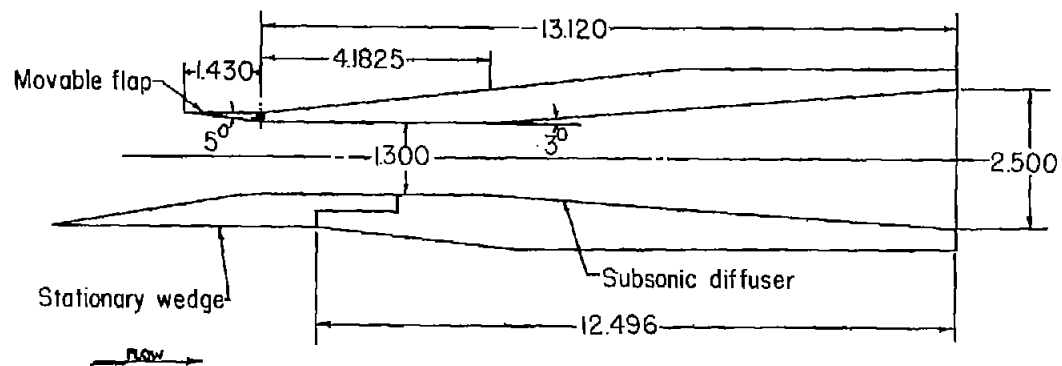
3. A 50-percent decrease in length of the subsonic diffuser of the inlet configuration that attained maximum total-pressure recovery for a design Mach number of 2.0 resulted in a 10-percent decrease in maximum total-pressure recovery.

4. Shadowgraphs of the forward portion of the inlets indicated extensive separation for the maximum-pressure-recovery case; thus, it appears that boundary-layer control is necessary to approach theoretical values of pressure recovery.

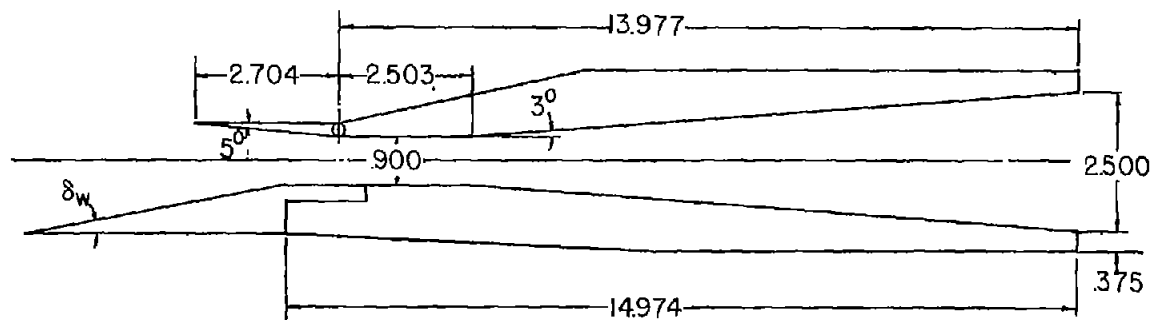
Langley Aeronautical Laboratory,
National Advisory Committee for Aeronautics,
Langley Field, Va., March 29, 1954.

REFERENCES

1. Kantrowitz, Arthur, and Donaldson, Coleman duP.: Preliminary Investigation of Supersonic Diffusers. NACA ACR L5D20, 1945.
2. Ferri, Antonio, and Nucci, Louis M.: Preliminary Investigation of a New Type of Supersonic Inlet. NACA Rep. 1104, 1952. (Supersedes NACA TN 2286.)
3. Evvard, John C., and Blakey, John W.: The Use of Perforated Inlets for Efficient Supersonic Diffusion (Revised). NACA RM E51B10, 1951.
4. Weinstein, Maynard I.: Performance of Supersonic Scoop Inlets. NACA RM E52A22, 1952.

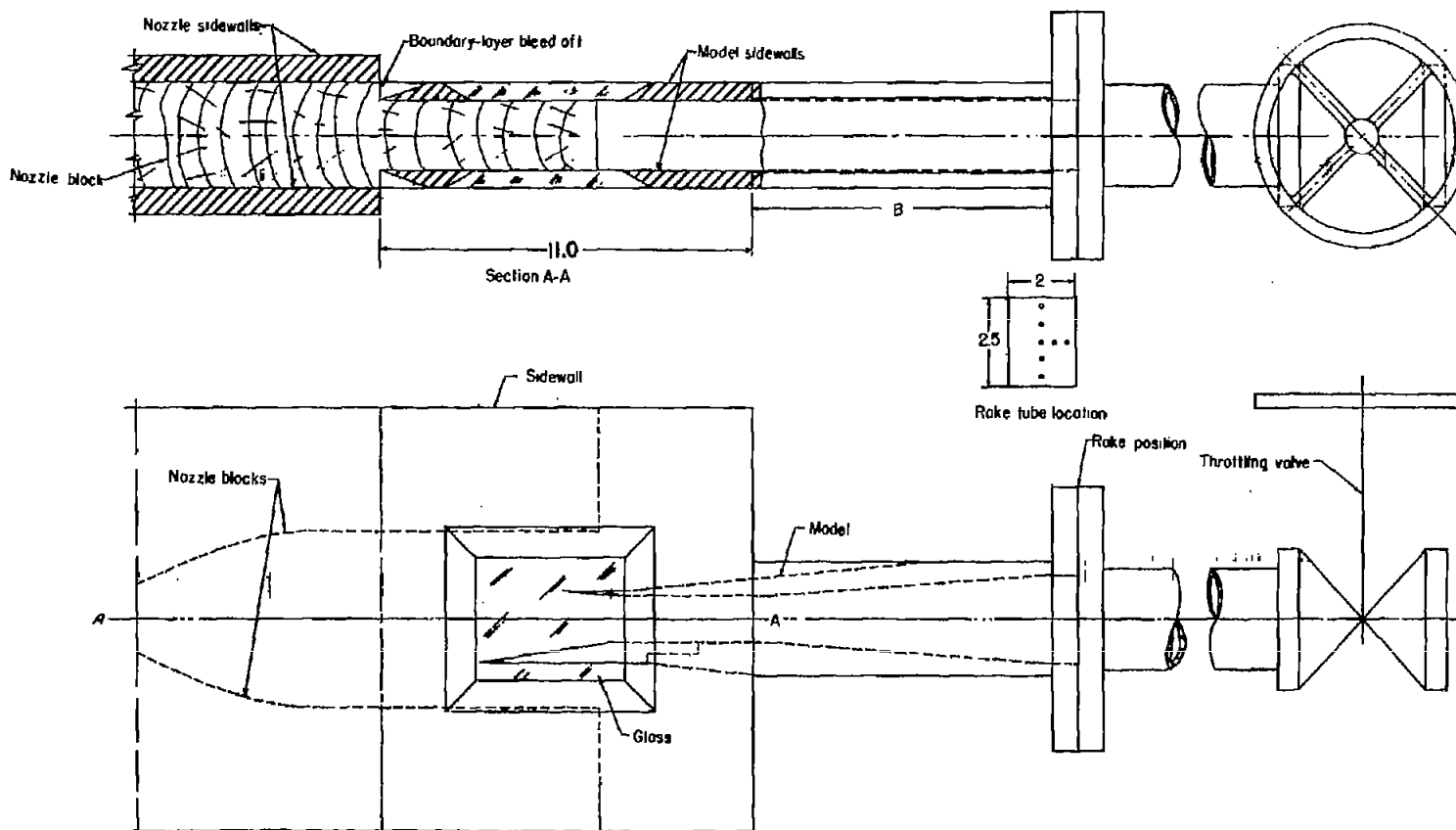


(a) Model 1.



(b) Model 2.

Figure 1.- Assembly drawing of two-dimensional inlet test arrangement.
All dimensions are in inches unless otherwise noted.



(c) Complete assembly.

Figure 1.- Continued.



(d) Side-view photograph of model 1A.

L-59817

Figure 1.- Concluded.

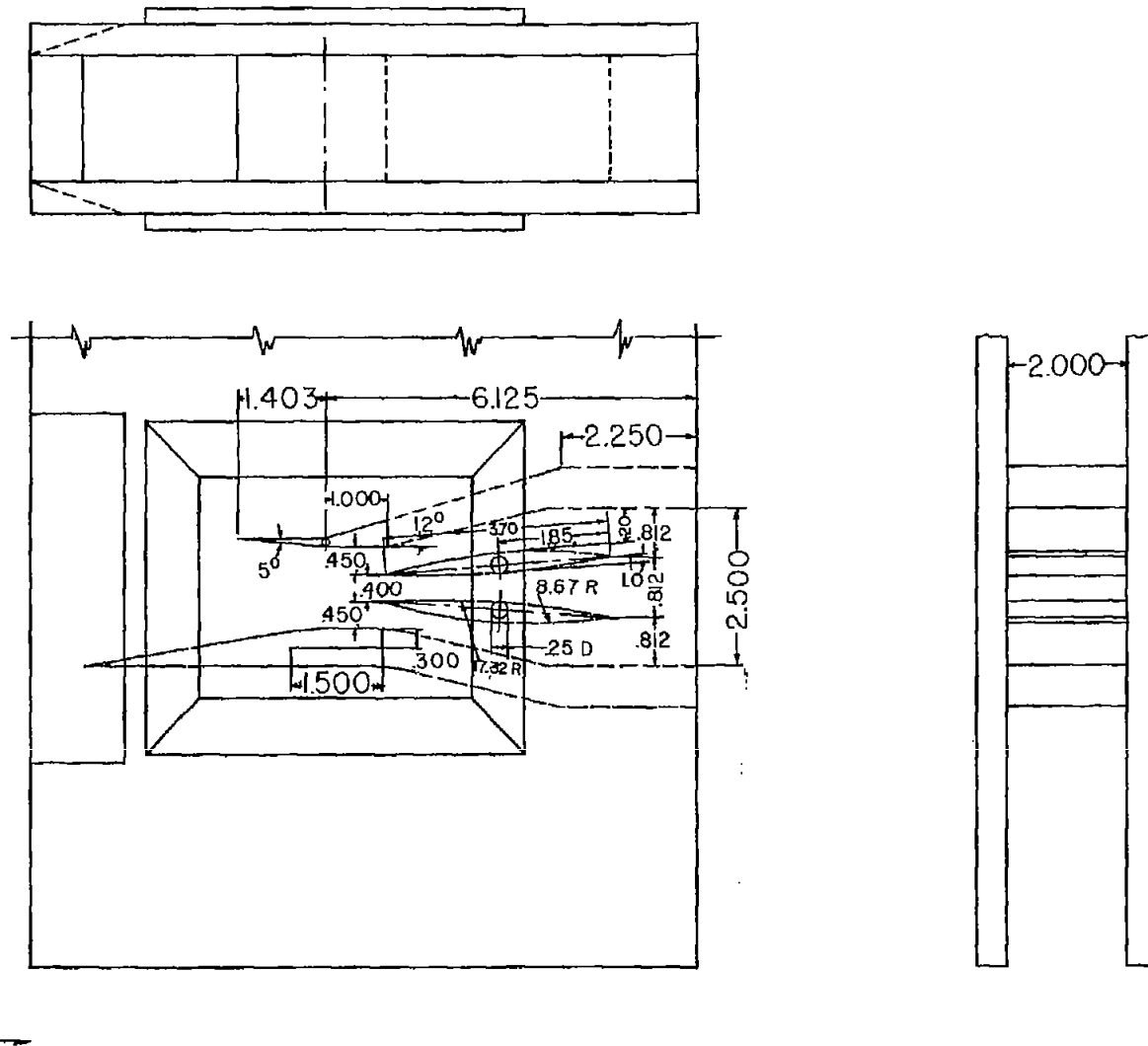


Figure 2.- Schematic drawing of short diffuser model. All dimensions are in inches.

CONFIDENTIAL

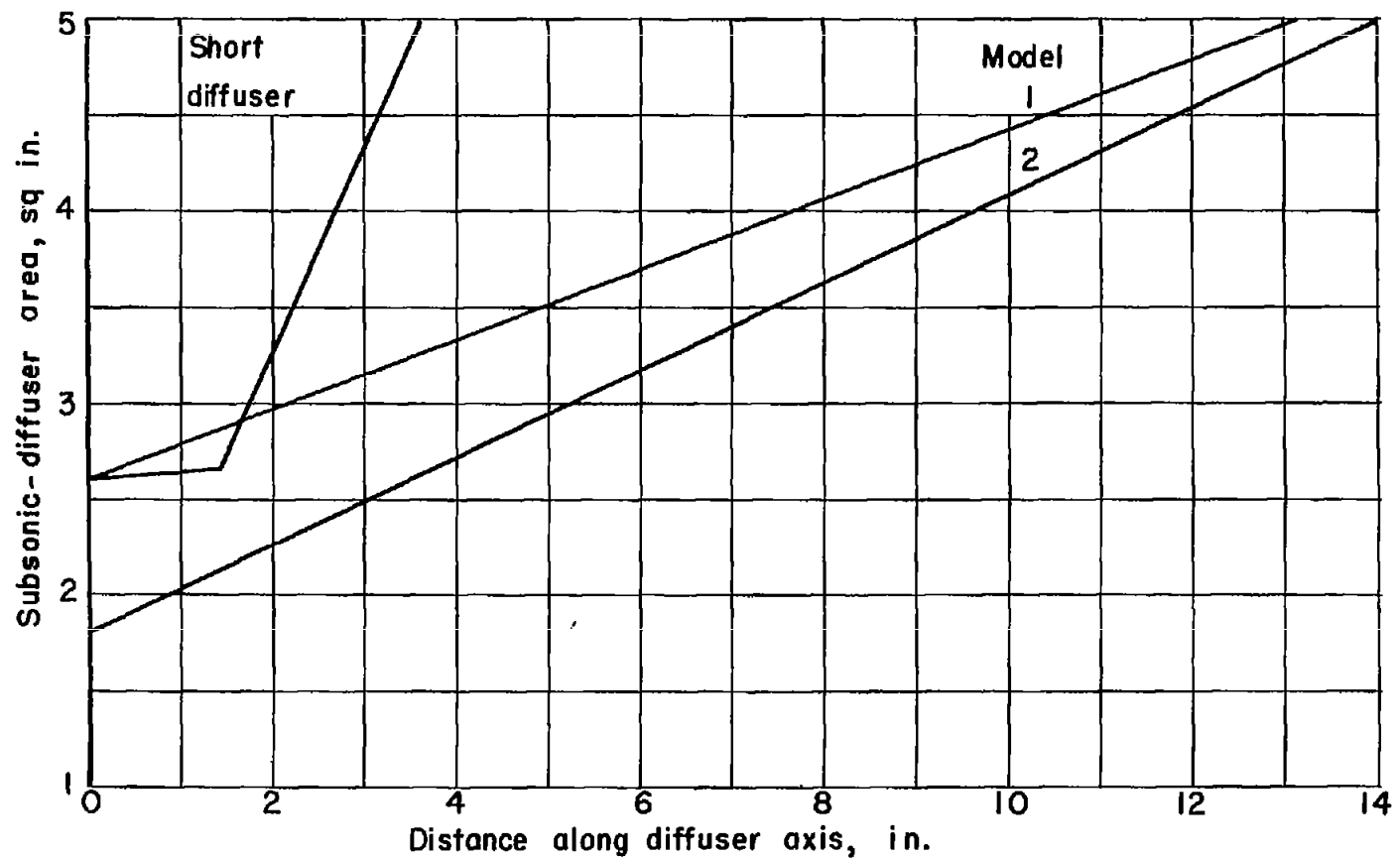


Figure 3.- Area distribution of subsonic diffuser section for models investigated.

CONFIDENTIAL

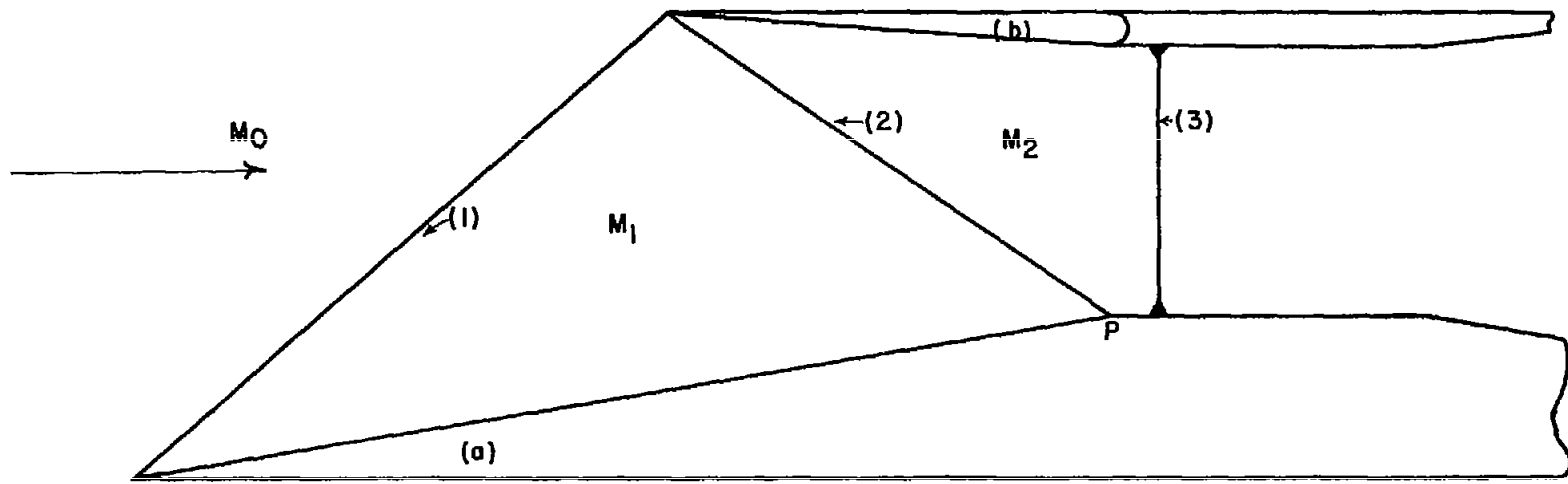
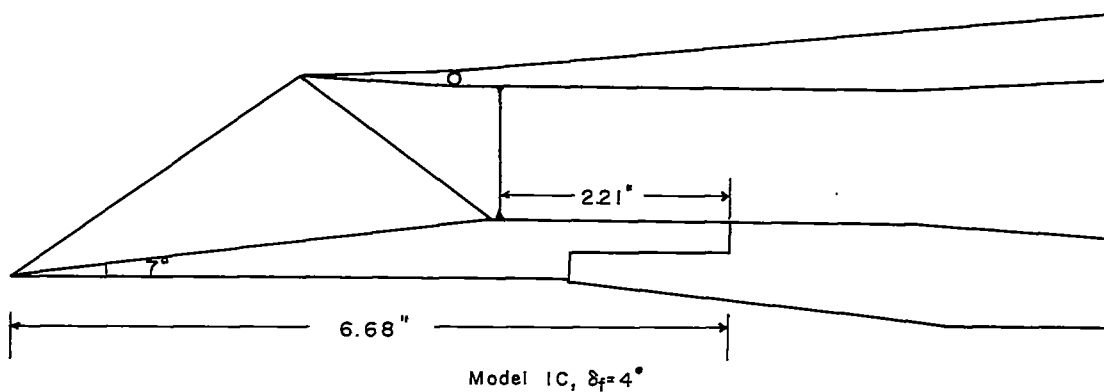
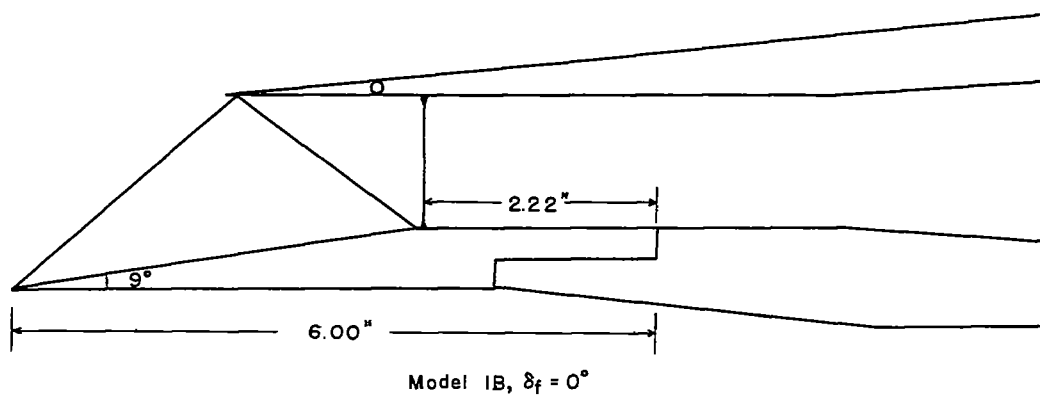
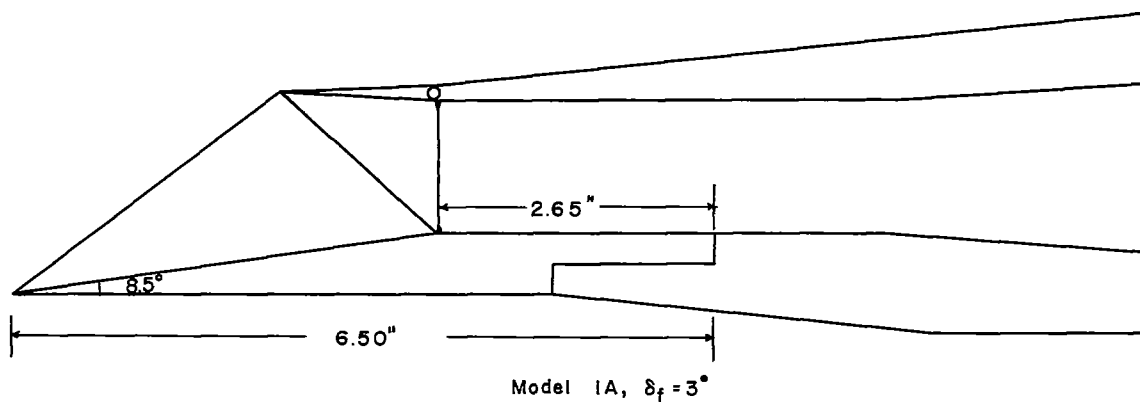
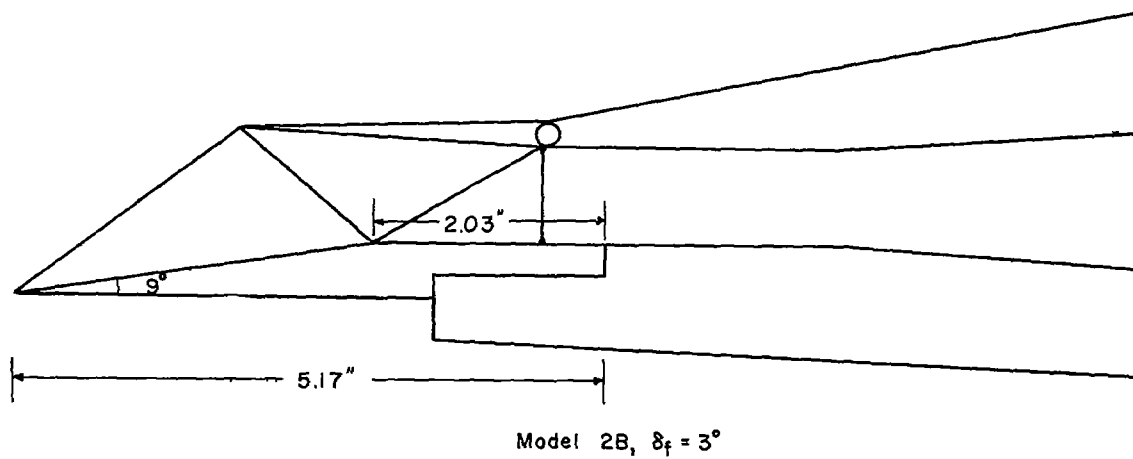
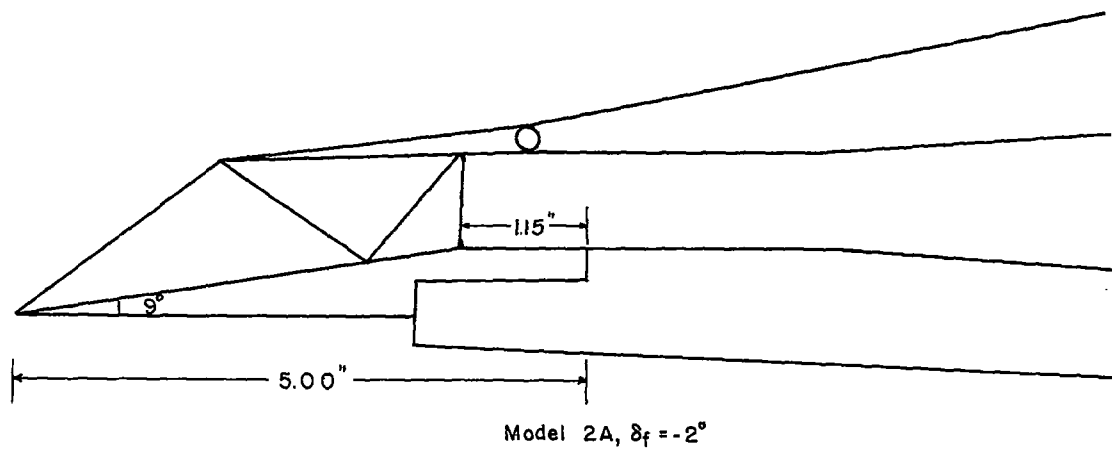


Figure 4.- General design criteria for the two-dimensional inlets.



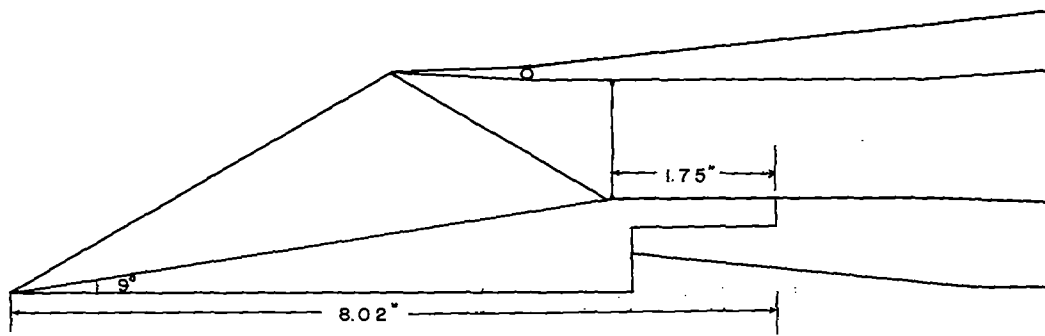
(a) $M = 2.0$.

Figure 5.- Design shock-wave patterns and stationary-wedge geometry for all two-dimensional inlets investigated.

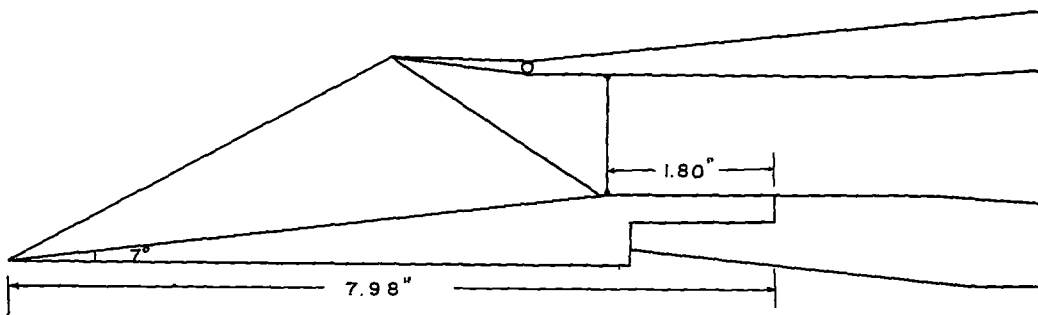


(a) Continued.

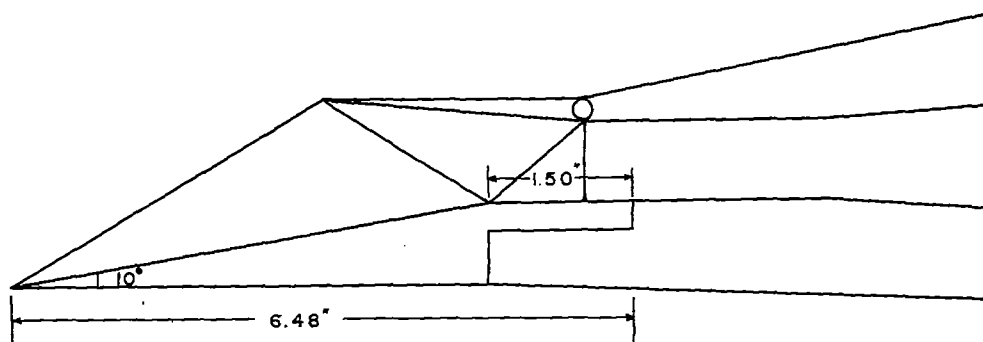
Figure 5.- Continued.



Model 1D, $\delta_f = 4^\circ$



Model 1E, $\delta_f = 7^\circ$



Model 2C, $\delta_f = 5^\circ$

(b) $M_D = 2.50$.

Figure 5.- Concluded.

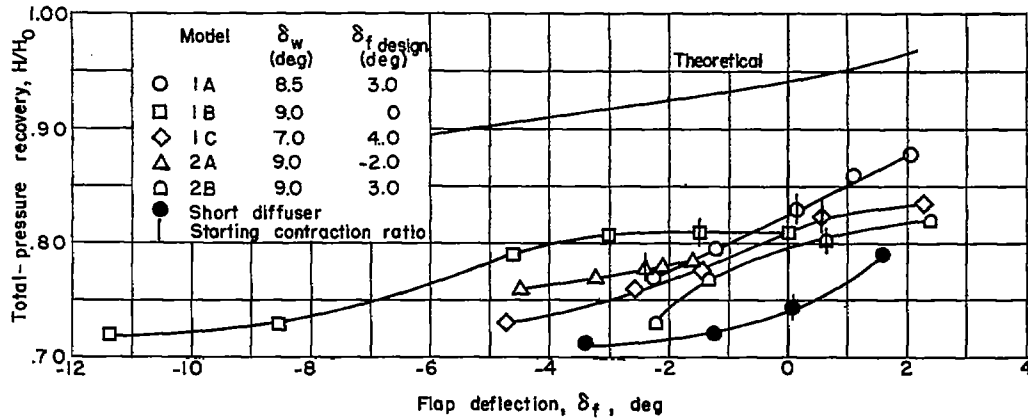


Figure 6.- Effect of flap deflection on the pressure-recovery characteristics of two-dimensional inlets designed for and tested at $M = 2.01$.

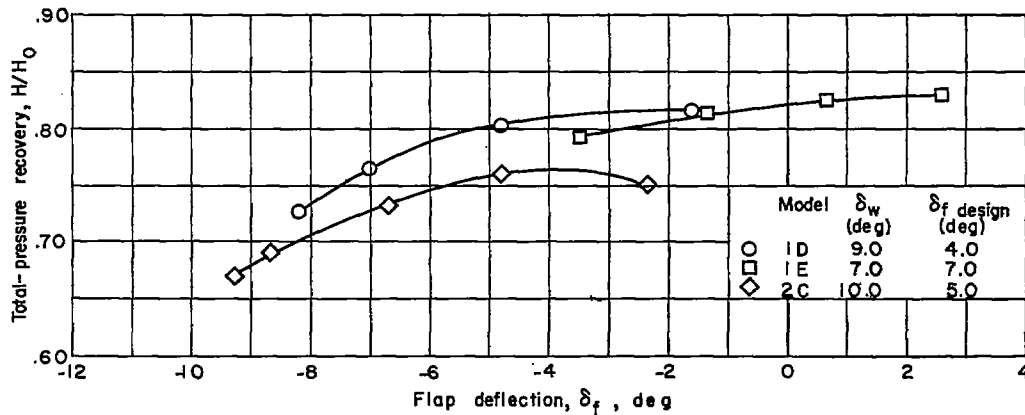
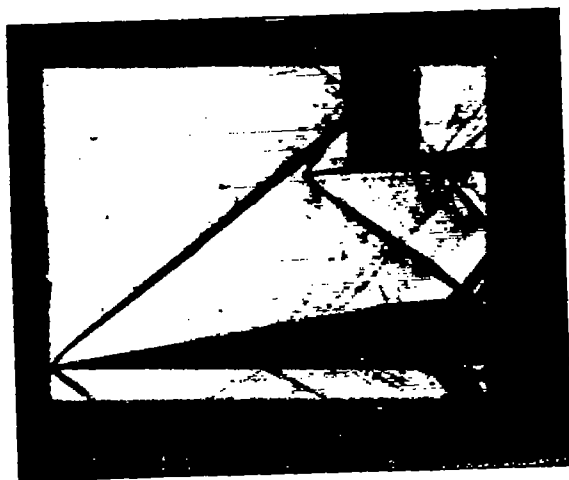
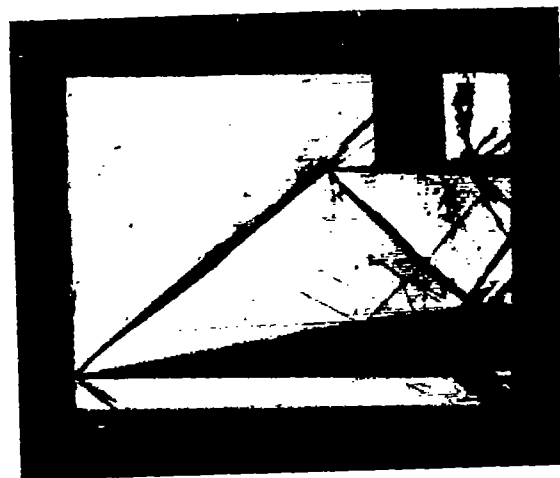


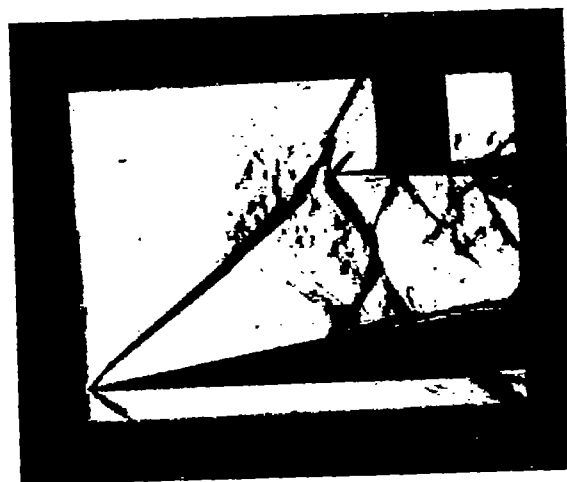
Figure 7.- Effect of flap deflection on the pressure-recovery characteristics of two-dimensional inlets designed for $M_D = 2.5$ and tested at $M = 2.01$.



(1) $\delta_f \approx 0^\circ$



(2) $\delta_f \approx 2^\circ$

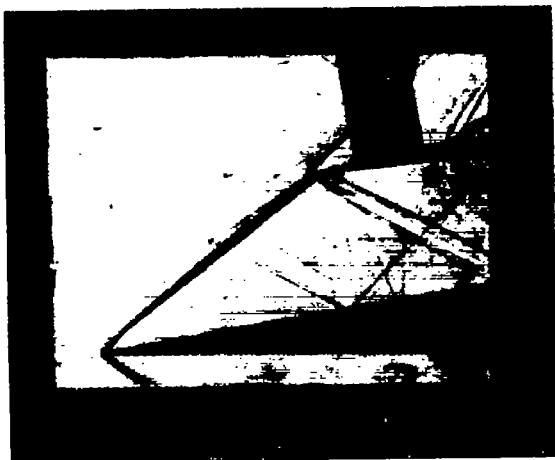
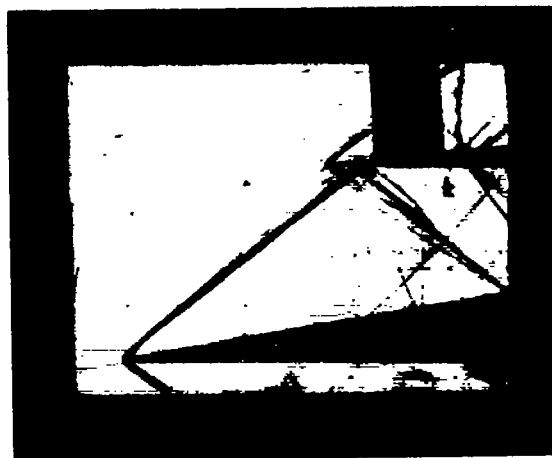
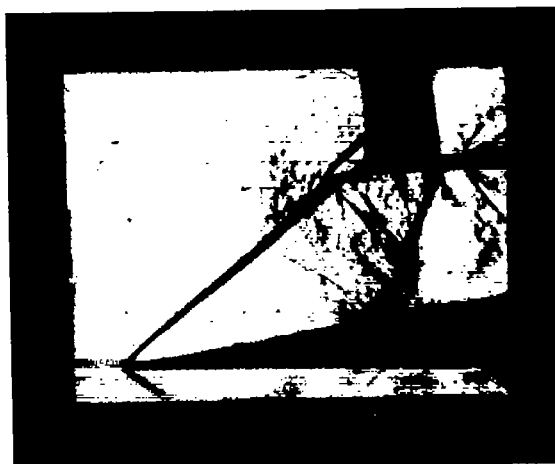


(3) $\delta_f \approx 2^\circ$

(a) Model 1A. $M_D = 2.0$.

L-83636

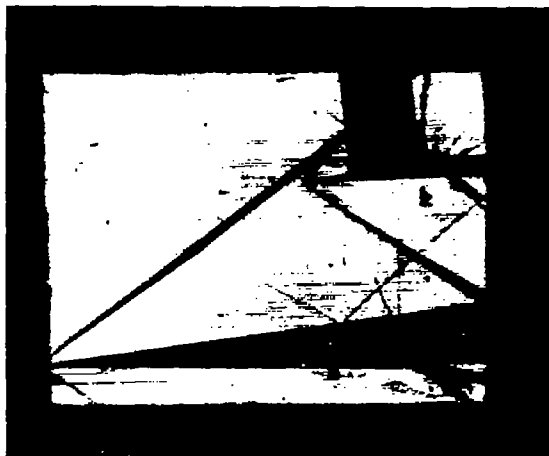
Figure 8.- Shadowgraphs of model 1. $M = 2.01$.

(1) $\delta_f \approx -5^\circ$ (2) $\delta_f \approx 1^\circ$ (3) $\delta_f \approx 1^\circ$

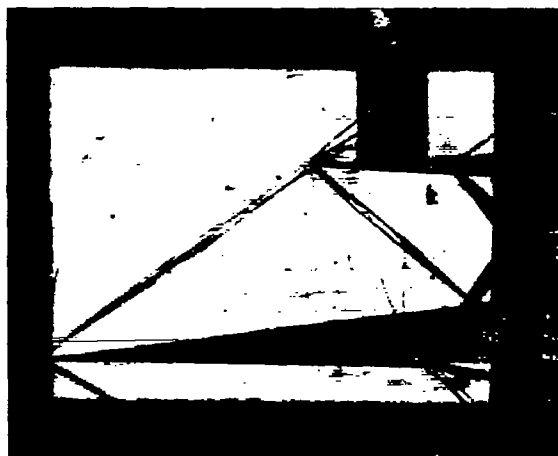
(b) Model 1B. $M_D = 2.0$.

L-83637

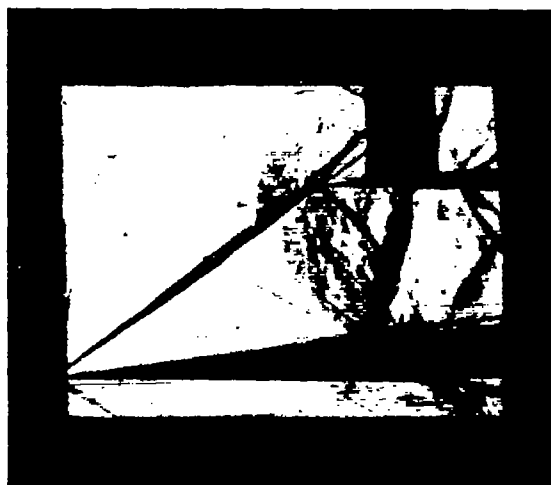
Figure 8.- Continued.



(1) $\delta_f \approx -1^\circ$



(2) $\delta_f \approx 2^\circ$

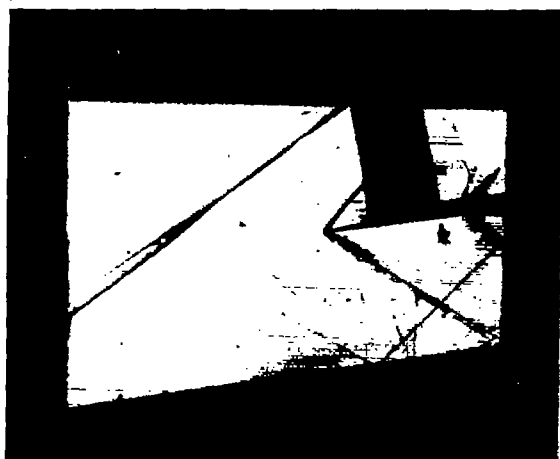
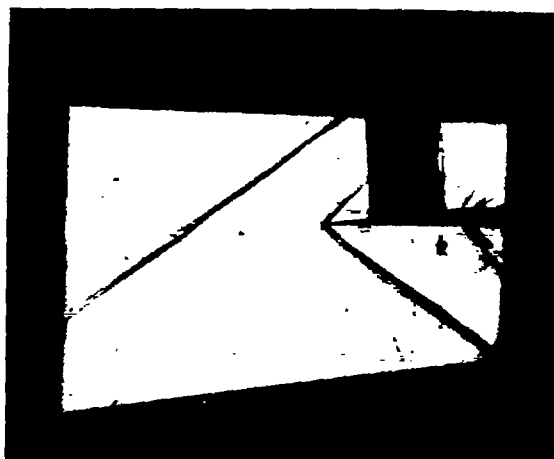


(3) $\delta_f \approx 2^\circ$

(c) Model 1C. $M_D = 2.0$.

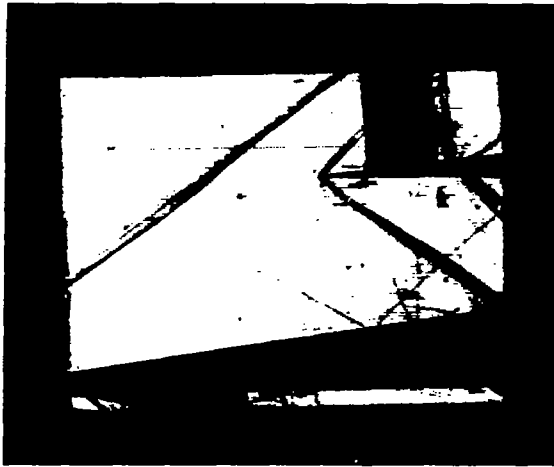
L-83638

Figure 8.- Continued.

(1) $\delta_f \approx -7^\circ$ (2) $\delta_f \approx -1.5^\circ$ (3) $\delta_f \approx -1.5^\circ$ (d) Model 1D. $M_D = 2.5$.

L-83639

Figure 8.- Continued.



(1) $\delta_f \approx 0^\circ$



(2) $\delta_f \approx 2.5^\circ$

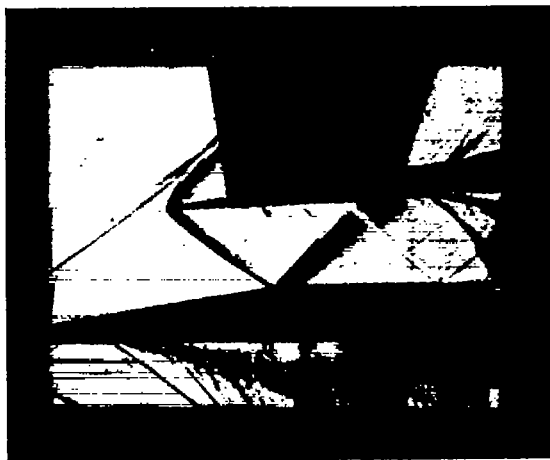
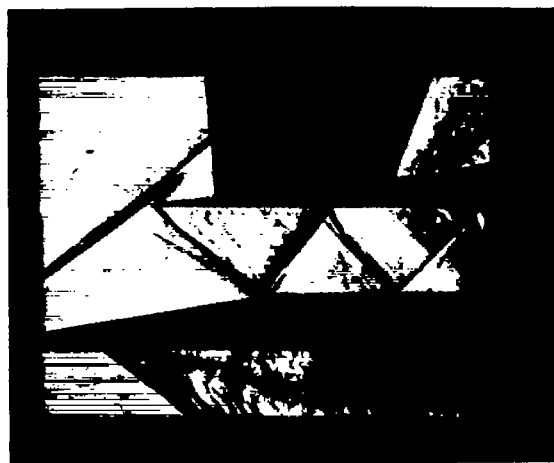


(3) $\delta_f \approx 2.5^\circ$

(e) Model 1E. $M_D = 2.5$.

L-83640

Figure 8.- Concluded.

(1) $\delta_f \approx -4^\circ$ (2) $\delta_f \approx -2.5^\circ$ (3) $\delta_f \approx -2.5^\circ$ (a) Model 2B. $M_D = 2.0$.

L-83641

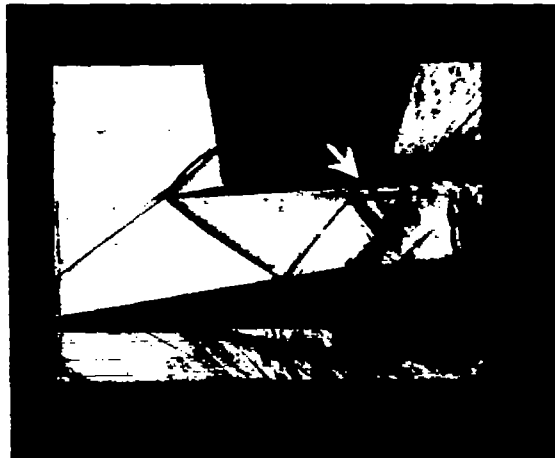
Figure 9.- Shadowgraphs of model 2. $M = 2.01$.



(1) Minimum back pressure.



(2) Low back pressure.

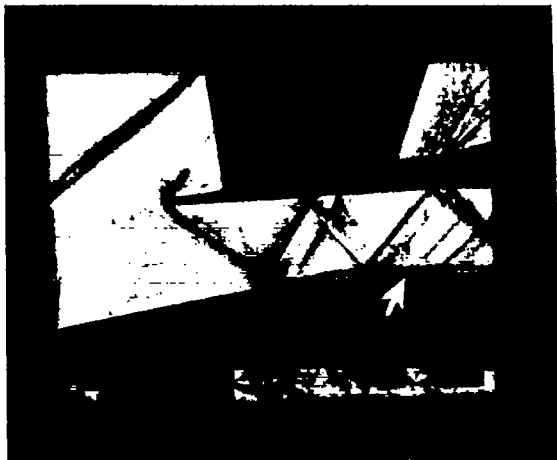


(3) High back pressure.

(b) Model 2A. $M_D = 2.0$.

L-83642

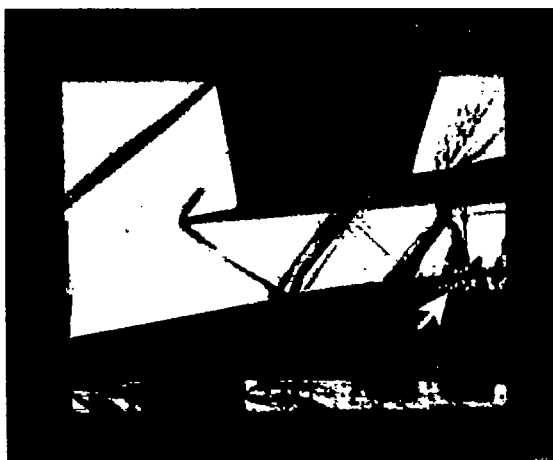
Figure 9.- Continued.



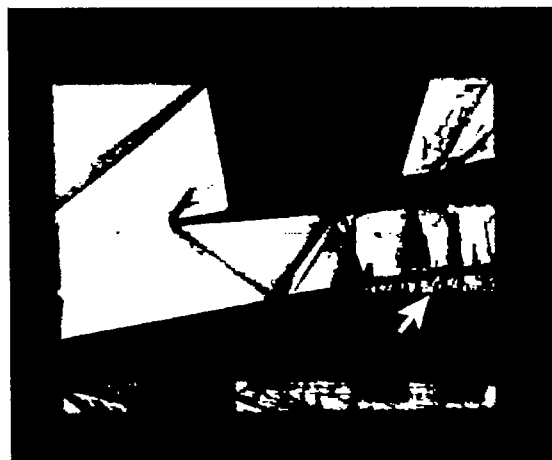
(1) Minimum back pressure.



(2) Low back pressure.



(3) High back pressure.



(4) Higher back pressure.

(c) Model 2C. $M_D = 2.5$.

L-83643

Figure 9.- Concluded.



(a) Low back pressure.



(b) High back pressure.

L-83644

Figure 10.- Shadowgraphs of short diffuser model. $M = 2.01$.

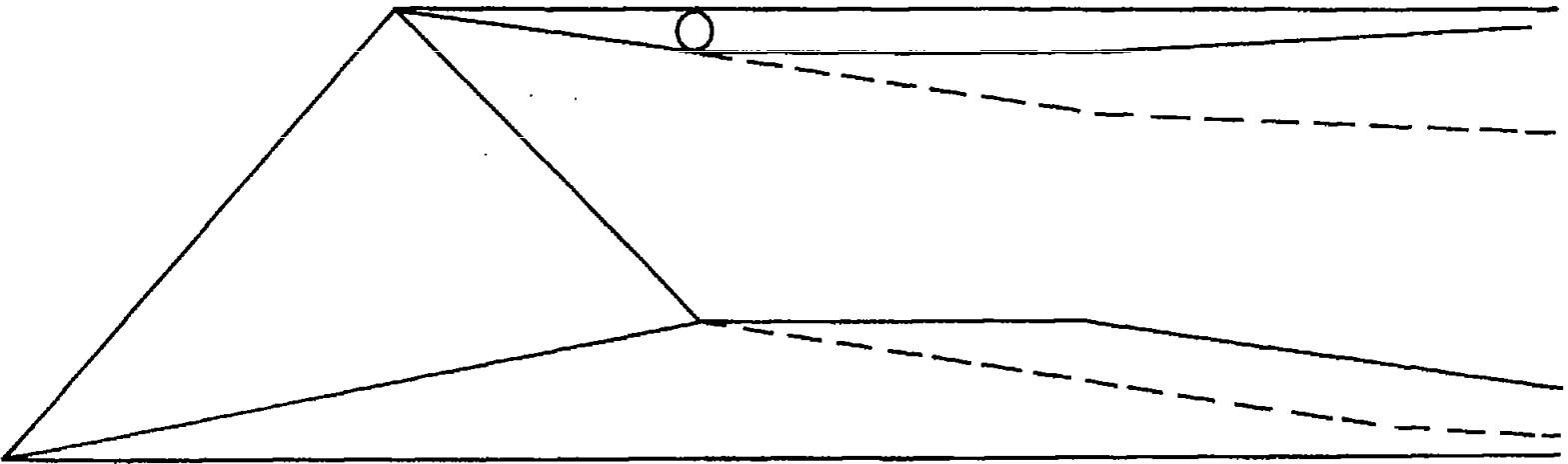


Figure 11.- Two-dimensional inlet modification.